CHEMISTRY OF MATERIALS
Cite This: Chem. Mater. 2018, 30, 2424−2435
Article
pubs.acs.org/cm

# Versatile Surface Modification of Cellulose Fibers and Cellulose Nanocrystals through Modular Triazinyl Chemistry

Ayodele Fatona,[†] Richard M. Berry,[‡] Michael A. Brook,[†] and Jose M. Moran-Mirabal*[,†]

[†]Department of Chemistry and Chemical Biology, McMaster University, 1280 Main Street West, Hamilton, Ontario L8S 4M1, Canada

[‡]Celluforce Inc., 625 President-Kennedy Avenue, Montreal, Quebec H3A 1K2, Canada

Supporting Information

**ABSTRACT:** The ability to tune the interfacial and functional properties of cellulose nanomaterials has been identified as a critical step for the full utilization of nanocellulose in the development of new materials. Here, we use triazine chemistry in a modular approach to install various functionalities and chemistries onto cellulose fibers and cellulose nanocrystals (CNCs). The surface modification is demonstrated in aqueous and organic media. Octadecyl, monoallyl-PEG, benzyl, and propargyl triazinyl derivatives were grafted onto cellulose/CNCs via aromatic nucleophilic substitution in the presence of base as hydrochloric acid scavenger. The covalent nature and degree of substitution of grafted aliphatic, polymeric, alkyne chains, and aromatic rings were characterized through Fourier transform infrared spectroscopy, X-ray photoelectron spectroscopy, elemental analysis, and thermogravimetric analysis. In addition, AFM and DLS analysis showed minimal change in the geometry and individualized character of CNCs after surface modification. X-ray diffraction analysis confirmed that the modification happened only at the CNC surface, while the bulk crystalline core remained unmodified. Modified cellulose/CNCs showed hydrophilic or hydrophobic properties depending on the grafted functionality, which resulted in stable colloidal suspensions of CNCs in polar and nonpolar organic solvents. Furthermore, the reactive nature of propargyl-modified cellulose was demonstrated by the successful grafting of an azido-fluorescein dye via copper-catalyzed Huisgen 1,3-dipolar cycloaddition. The triazinyl chemistry thus presents a versatile route for tuning the interfacial properties of nanocellulose, with the possibility of postmodification for applications that require the conjugation of molecules onto cellulose through bio-orthogonal chemistries.

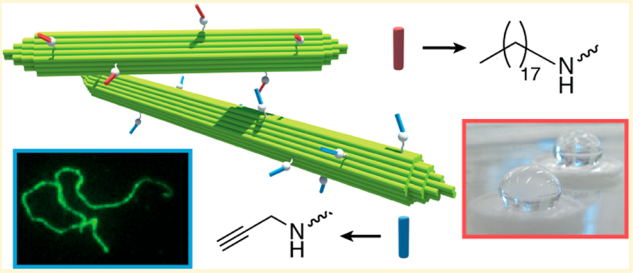


## INTRODUCTION

Cellulose is an attractive green material due to its intrinsic mechanical and chemical properties, which can be used to build hierarchical structures that enhance the performance of traditional polymeric materials.[1−3] The partial hydrolysis of the networks of cellulose microfibrils in plant cell walls with strong acids, which attack preferentially the disordered or paracrystalline regions of the microfibrils, allows the isolation of highly crystalline rodlike nanoparticles, called cellulose nanocrystals (CNCs). These environmentally friendly and noncytotoxic[4] nanoparticles have unique characteristics, including very high surface area (150−300 $m^2 g^{-1}$),[5,6] high tensile strength (7.5−7.7 GPa),[7] high elastic modulus (110−220 GPa),[7] high aspect ratio (∼20−70),[5] and interesting optical and electrical properties.[8] Such characteristics make them attractive for a broad range of applications, including materials reinforcement, drug delivery, foam stabilization, supercapacitor development, and rheological property modification, among many others. However, a major hurdle to the widespread application and utilization of CNCs, and nanocellulose in general, is their inability to form stable suspensions in a range of organic solvents or be compatible with polymer matrices. Thus, the effective use of CNCs in select applications, such as materials reinforcement, depends strongly on our ability to tune their interfacial properties to enhance dispersion or introduce reactive functional groups that can form covalent bonds with the host matrix.

The surface chemistry of isolated CNCs is dependent on the acid used during hydrolysis. Sulfuric acid hydrolysis of cellulose is still the most common process for CNC isolation and results in the grafting of sulfate half-ester groups onto the surface of the isolated CNCs. While these negatively charged groups allow the colloidal stabilization of CNCs in aqueous media through electrostatic repulsion, they, along with the abundant hydroxyl groups on the CNC surface, prevent their suspension/dispersion in most organic solvents and polymer systems.[5,9] This limits the reinforcement capabilities of CNCs as well as their processability for new nanotechnological applications.

Efforts have been made to convert electrostatically stabilized CNCs into sterically stabilized CNCs through the modification of the surface-reactive hydroxyl groups along the cellulose backbone. This would permit the CNCs to be dispersed in nonaqueous solvents and enhance their compatibility with a wide

Received: February 3, 2018
Revised: March 16, 2018
Published: March 16, 2018





DOI: 10.1021/acs.chemmater.8b00511
Chem. Mater. 2018, 30, 2424−2435

range of hydrophobic polymer matrices. Esterification,[10] cationization,[11] carbamination,[12−14] silylation,[15] amidation,[16,17] polymer grafting,[18,19] and etherification[20] have all been successfully used to modify the surface of CNCs. However, such approaches are rarely suitable for large-scale implementation or have limitations in the functionalities that can be introduced. The present work explores triazine chemistry—a well-known technology in the textile, agriculture, polymer, and paper industries for the production of dyes,[21] herbicides,[22] optical brighteners,[23] and dendrimers[24]—as a simple, versatile, and mild approach to carry out the modular surface modification of cellulose, especially CNCs, with potential for large-scale implementation. Haller and Heckendorn[21] pioneered the triazine chemistry for affixing amino-reactive dyes onto cellulose fibers for coloration. Helbert et al.,[25] Ringot et al.,[26] and Walczak et al.[27] further extended this process for the grafting of fluorescent dyes, porphyrin, and *N*-lipidated oligopeptides onto cellulose fibers, for applications involving the study of cellulase activity, endowing cellulose with antibacterial properties, and for metabolite profiling, respectively.

Our choice of 2,4,6-trichloro-1,3,5-triazine (cyanuric chloride) as a linker molecule derives not only from its commercial availability and low cost, but also from the ease of derivatizing cyanuric chloride with nucleophiles to generate a myriad of mono- or disubstituted 1,3,5-triazines. In our approach, the surface functionality of CNCs is strategically tuned by first grafting the targeted molecules (small or polymeric) onto the cyanuric chloride linker, and then grafting the resulting triazinyl derivatives onto CNCs in a single step. In this way, the triazinyl linker can be used either as a standalone modification or as a building block for secondary modifications with biorthogonal chemistries. An additional advantage of this chemistry is that the selective chlorine substitution of cyanuric chloride can be controlled with moderate temperatures, making it a highly predictable procedure for nanocellulose modification. More importantly, to the best of our knowledge, this is the first article detailing the use of triazine chemistry in tuning the interfacial properties of nanocellulose.

We report the grafting of four different triazinyl derivatives onto crystalline cellulose fibers or CNCs. These consist of nonpolar aliphatic chains (octadecylamine, C18), polymer chains (poly(ethylene glycol) mono allyl ether, APEG), aromatic rings (benzylamine), and alkyne functionalities (propargylamine). Depending on the chemical moiety coupled to cyanuric chloride, the surface modification of CNCs was carried out in polar or nonpolar solvents. With this chemistry, the polarity of the CNC surface has been tuned to enable their dispersion in a range of solvents to form homogeneous colloidal suspensions that are stabilized through electrostatic and steric interactions. In addition, two triazine derivatives are amenable to further addition chemistries such as click reactions. Thus, as proof-of-concept, nanocellulose modified with propargyl-triazine derivatives was further modified with fluorescein through an azide−alkyne click reaction.

Our intention is to leverage the triazine chemistry as a versatile and low-cost technique for surface modification of CNCs. It is anticipated that this surface chemistry will aid in the production of functional CNCs that can be deployed in high-volume nanocomposite processing, rheological modification, cosmetics, and sensing applications.

## EXPERIMENTAL SECTION

**Materials.** Octadecylamine (C18), benzylamine, propargylamine, cyanuric chloride, triethylamine, *N*,*N*-diisopropylethylamine (DIPEA), sodium hydroxide (NaOH), Whatman grade 1 cellulose filter paper (10 mm), and potassium carbonate ($K_2CO_3$) were purchased from Sigma-Aldrich (Oakville, ON, Canada). Poly(ethylene glycol) monoallyl ether (MW 388 g $mol^{-1}$) was a gift from EnRoute Interfaces, Inc. (Hamilton, ON, Canada). 5-Fluorescein azide (5-FAM-Azide) was purchased from Lumiprobe Corp. (Hunt Valley, MD). Spray-dried cellulose nanocrystals hydrogen sulfate sodium salt (CNCs) were provided by CelluForce Inc. (Montreal, QC, Canada). All solvents including dichloromethane (DCM), acetone, ethanol, *N*,*N*-dimethylformamide (DMF), tetrahydrofuran (THF), and chloroform were purchased from Caledon Laboratories (ON, Canada) and used as received. Bacterial microcrystalline cellulose (BMCC) was isolated in house from the commercial foodstuff Nata de Coco.

**Characterization: Nuclear Magnetic Resonance (NMR).** ($^1$H and $^{13}$C NMR) spectra were obtained on a Bruker AV600-600 MHz NMR spectrometer using deuterated $CDCl_3$ and $CD_2Cl_2$ as solvents.

**Mass Spectrometry (MS).** Mass spectra of synthesized dichlorotriazinyl derivatives were recorded on a Micromass Ultima (LC-ESI/APCI) Triple Quadrupole mass spectrometer and Micromass Global Ultima ESI Quadrupole Time of Flight (Q-TOF) mass spectrometer.

**Fourier Transform Infrared Spectroscopy (FTIR).** FTIR spectra of unmodified and modified CNCs were recorded on a Thermo Nicolet 6700 FTIR spectrometer in transmission mode using KBr disks loaded with 1 wt % sample dried under vacuum overnight at 60 °C.

**X-ray Photoelectron Spectroscopy (XPS).** Spectra were recorded with a Thermo Scientific Theta Probe XPS spectrometer with monochromatic Al K$\alpha$ radiation (50 W) at a takeoff angle of 45° and a spot size of 200 $\mu$m. Survey and high-resolution spectra were collected with pass energies of 280 and 26 eV, respectively, and data were analyzed with the software provided with the instrument. Unmodified and modified CNC samples, 1 wt %, were deposited via drop casting onto clean silicon wafers and air-dried at room temperature before analysis.

**Elemental Analysis.** Mass fractions of carbon, hydrogen, nitrogen, and sulfur were determined for vacuum-dried unmodified and modified CNCs by Micro Analysis Inc. (Wilmington, DE). The samples were combusted in a pure oxygen environment where product gases were separated and detected by thermal conductivity. Triplicates were measured for each sample, and averages are reported. The results obtained from this technique were used to determine the degree of substitution (DS), given by the number of hydroxyl groups substituted by dichlorotriazinyl derivatives per unit of anhydroglucose. The DS was calculated using eq 1 below; as reported[28]

$$(\mathrm{DS}) = \frac{72.07 - C \times 162.14}{M_g \times C - M_{C_g}} \quad (1)$$

where $C$ is the relative carbon content in the sample; the numbers 72.07 and 162.14 correspond to the carbon mass of the anhydroglucose unit ($C_6H_{10}O_5$) and the molecular weight of anhydroglucose, respectively; $M_g$ and $M_{C_g}$ correspond to the molecular weight of the dichlorotriazinyl derivatives (i.e., compounds **1**, **2**, **3**, and **4**) linked to the anhydroglucose unit, and their carbon masses, respectively. Experimental values were corrected by a conversion factor of 1.077 considering unmodified CNCs as pure cellulose, which correlates with a relative carbon content of 44.44%, following a previously reported procedure.[29]

**Thermogravimetric Analysis (TGA).** Analyses were carried out on a TA Instruments Q50 thermogravimetric analyzer. Data were collected after placing ca. 10 mg of a vacuum-dried sample in a clean platinum pan and heating from ambient temperature to 800 °C under argon atmosphere (heating rate of 20 °C $min^{-1}$).

**Fluorescence Microscopy.** Fluorescence images of BMCC labeled using triazine-alkyne−azide click chemistry were taken using a Nikon-Eclipse LV100N POL microscope, equipped with excitation and emission filters for fluorescein dye, a Retiga 2000R CCD monochromatic camera (QImaging, Surrey, BC, Canada), and CFI LU P


DOI: 10.1021/acs.chemmater.8b00511
*Chem. Mater.* 2018, 30, 2424−2435

**Scheme 1. (A) Synthesis of 4,6-Dichloro-1,3,5-triazine Derivatives, (B) Chemical Grafting of 4,6-Dichloro-1,3,5-triazine Derivatives onto Cellulose, and (C) Fluorescein Azide Click Grafting onto Alkyne-Modified Nanocellulose**

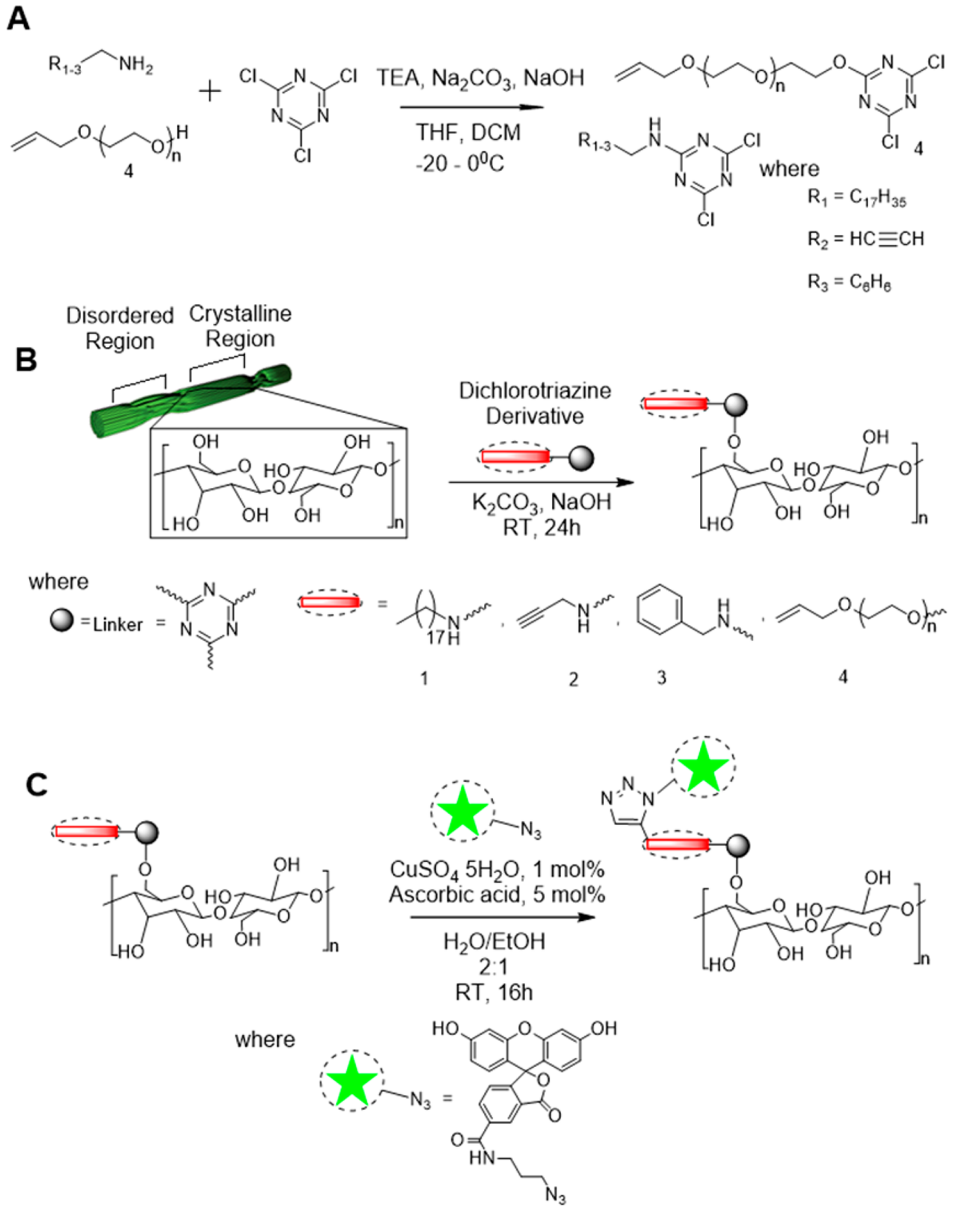


10×/0.25 NA and 40×/0.65 NA objectives (Nikon Canada Inc., Mississauga, ON, Canada).

**Dynamic Light Scattering (DLS).** The apparent hydrodynamic size was measured for native and surface-modified CNCs in 0.025 wt % dispersions in water (except for **DTC18**-modified CNCs, where the measurements were done in 1:1 chloroform:DMSO) using a Malvern Zetasizer Nano particle analyzer. Triplicate samples were measured 15 times each, and the average hydrodynamic size is reported. The standard deviation from the triplicate samples is reported as the error for the measurements.

**Atomic Force Microscopy (AFM).** AFM images were obtained using an Asylum Research MFP-3D ClassicTM scanning probe microscope (Santa Barbara, CA). Images were acquired in tapping mode with aluminum reflex coated silicon cantilevers (FMR, Nanoworld AG, Neuchâtel, Switzerland) with nominal spring constant of 2.8 N $m^{-1}$ and resonant frequency of 75 kHz. Samples were prepared by spin coating solutions containing 0.001 wt % unmodified CNCs or 0.01 wt % modified CNCs samples onto piranha-cleaned silicon wafers (for unmodified CNCs, the substrates were pretreated by spin coating with a 0.1% PAH solution) at 4000 rpm for 30 s and air-dried at room temperature before analysis. CNC lengths were measured for individual particles within the images, and an average was calculated for $n > 50$ measurements. The error associated with the CNC lengths is reported as the standard deviation of the measurements.

**X-ray Diffraction (XRD).** Two-dimensional diffraction patterns were collected using a D8 Davinci diffractometer (Bruker, Billerica, MA) equipped with a sealed tube cobalt source. Analysis of the resulting patterns was conducted using the Bruker TOPAS software and Matlab scripts. The beam was collimated to a diameter of 0.5 mm (35 mA, 45 kV). Cellulose samples were drop-cast and oven-dried onto clean Si wafer pieces for the analysis. A still frame of a blank piece of Si was initially examined to correct for background. The background intensity was subtracted from each sample frame prior to integration of the data. A $2\theta$ range 13−42° was used for the crystallinity index (CrI) analysis. Integration along relative angle $\chi$ for every $2\theta$ value was performed to obtain one-dimensional diffraction plots of intensity versus $2\theta$. The background corrected intensity versus $2\theta$ plots were fitted to five symmetric Lorentzian peaks; four peaks corresponding to the (100), (010), (002), and (040) crystalline planes,[30] and one broad amorphous peak fixed at 24.1°. The CrI was calculated by the peak deconvolution



DOI: 10.1021/acs.chemmater.8b00511
*Chem. Mater.* 2018, 30, 2424−2435

method as the ratio of the area for the crystalline peaks over the total area for the diffraction plots.

**Contact Angle Measurements.** The wettability values of modified cellulose fibers (Whatman filter paper) were assessed by static contact angle measurement through sessile drop method via an OCA 20 Future Digital Scientific system (Garden City, NY) equipped with a CCD camera. Water (1 $\mu$L of 18.2 MΩ $cm^{-1}$, A10-Merck-Millipore system, Darmstadt, Germany) was dropped onto modified cellulose paper while digital images were captured. The average of 3 replicate filter paper samples is reported as the contact angle.

**Synthesis of 4,6-Dichloro-*n*-octadecyl-1,3,5-triazine-2-amine (1, DTC18).** See Scheme 1a. $Na_2CO_3$ (2.86 g, 0.027 mol) was added to a stirred solution of cyanuric chloride (5.0 g, 0.027 mol) in dry THF (50 mL) cooled to 0 °C. After 20 min of stirring, a solution containing *n*-octadecylamine (7.28 g, 0.027 mol) in dry THF (100 mL) was added dropwise over a period of 45 min. The end of reaction—complete disappearance of starting material—was monitored via TLC (silica gel, DCM). The reaction mixture was filtered, and THF was removed under vacuum to yield a white precipitate which was suspended in water for 1 h to remove any remaining $Na_2CO_3$. This suspension was filtered, and the filtrate was dried at room temperature to give the final product (white precipitate, 10.9 g, 97% yield). $^1$H NMR (600 MHz, $CD_2Cl_2$, ppm) $\delta$: 5.96 (s, 1H), 3.51−3.38 (m, 2H), 1.69−1.58 (m, 2H), 1.43−1.23 (m, 31H), 0.90 (t, $J$ = 7.0 Hz, 3H). $^{13}$C NMR (151 MHz, $CD_2Cl_2$, ppm) $\delta$: 170.20, 166.53, 41.94, 32.32, 30.44, 27.01, 23.08, 14.26. HRMS (ESI-QTOF): calcd for $C_{21}H_{38}Cl_2N_4$, 417.46; found, 417.2543 ($M^+$).

**Synthesis of 4,6-Dichloro-*n*-propargyl-1,3,5-triazine-2-amine (2, DTP).** See Scheme 1a. Propargyl amine (0.59 g, 0.69 mL, 10.76 mmol) was added to a stirred solution of cyanuric chloride (2.00 g, 10.85 mmol) in dry THF (25 mL) cooled to −20 °C. DIPEA (1.54 g, 2.08 mL, 11.94 mmol) in dry THF (5 mL) was then added dropwise over a period of 2 h with the help of a syringe pump. Thereafter, reaction mixture was stirred for another 3 h maintaining the reaction temperature between −20 and 0 °C. After this time, THF was removed under vacuum to yield a residue that was dissolved in EtOAc (50 mL) in a separating funnel and washed with water (3 × 15 mL), followed by brine solution (30 mL) and finally dried over solid anhydrous $Na_2SO_4$ to yield a pure product (white precipitate) in quantitative yield (2.18 g, 99%) under reduced pressure. $^1$H NMR (600 MHz, $CDCl_3$, ppm) $\delta$: 6.00 (s, 1H), 4.23 (dd, $J$ = 5.7, 2.5 Hz, 2H), 2.26 (t, $J$ = 2.5 Hz, 1H). $^{13}$C NMR (151 MHz, $CD_2Cl_2$, ppm) $\delta$: 170.62, 166.10, 78.16, 72.73, 31.61. MS (ESI): calcd for $C_6H_4Cl_2N_4$, 203.03; found, 203.0 ($M^+$).

**Synthesis of 4,6-Dichloro-*n*-benzyl-1,3,5-triazine-2-amine (3, DTB).** See Scheme 1a. $Na_2CO_3$ (0.58 g, 5.4 mmol) was added to a stirred solution of cyanuric chloride (1.00 g, 5.4 mmol) in dry THF (20 mL) cooled to −20 °C. After 20 min of stirring, a solution containing benzylamine (0.58 g, 5.5 mmol) in dry THF (10 mL) was added dropwise over a period of 60 min. The end of reaction was monitored via TLC (silica gel, DCM). The product was isolated by centrifugation followed by filtration of the supernatant, and evaporation under vacuum to yield a pure product (white precipitate) in quantitative yield (1.35 g, 98%). $^1$H NMR (600 MHz, $CDCl_3$, ppm) $\delta$: 7.45−7.28 (m, 5H), 6.10 (s, 1H), 4.67 (d, $J$ = 6.0 Hz, 2H). $^{13}$C NMR (151 MHz, $CDCl_3$, ppm) $\delta$: 169.81, 165.50, 136.07, 129.03, 128.25, 127.76, 45.52. MS (ESI): calcd for $C_{10}H_8Cl_2N_4$, 255.10; found, 255.3 ($M^+$).

**Synthesis of 4,6-Dichloro-2-poly(ethylene glycol) monoallyl-1,3,5-triazine-2-ether (4, DTAPEG).** See Scheme 1a. Poly(ethylene glycol) monoallyl ether (4.21 g, 10.85 mmol) dissolved in DCM (20 mL) was added to a stirred solution of cyanuric chloride (2.00 g, 10.85 mmol) in DCM (30 mL) cooled to −20 °C. After 20 min of stirring, a NaOH solution (50%, 1 g in 2 mL of water) was added dropwise over 30 min with constant stirring. After 2 h of stirring while keeping temperature near 0 °C, the organic layer was separated and washed twice with water (2 × 10 mL), dried over $Na_2SO_4$ and concentrated under vacuum, resulting in an oily product (5.0 g, 86% yield). $^1$H NMR (600 MHz, $CDCl_3$, ppm) $\delta$: 5.99−5.84 (m, 1H), 5.31−5.12 (dd, 2H), 4.72−4.54 (m, 2H), 4.03 (d, $J$ = 5.5 Hz, 2H), 3.91−3.81 (m, 2H), 3.78−3.5 (m, 29H). $^{13}$C NMR (151 MHz, $CDCl_3$, ppm) $\delta$: 172.50, 171.06, 134.78, 117.07, 72.36, 71.32, 69.40, 68.42.

**Chemical Grafting of Dichlorotriazinyl Derivatives onto Nanocellulose.** See Scheme 1b. Two methods were used in the grafting of dichlorotriazinyl derivatives onto CNCs : In method 1, an aqueous suspension of CNCs (20 mL, 1 wt %) in a 100 mL round-bottomed flask was solvent-exchanged into DMF (30 mL) by vacuum-assisted rotary evaporation removing a small portion of water (10 mL). This was followed by successive centrifugation (10 000*g*, 5 °C, 10 min) and resuspension in acetone and then dry DCM, with sonication (10 min, 5 °C) in between each solvent-exchange step to prevent CNC aggregation. $K_2CO_3$ (0.25 g, 1.81 mmol) was added to a stirred suspension containing CNCs in dry DCM (0.5 g, 1 wt %). After 20 min, 5 mmol of **1**, **2**, or **3** (10:1 excess to the surface OH per g of CNCs) in dry DCM (10 mL) was added and left to stir at room temperature for 24 h. Modified CNCs were then subjected to 3 successive centrifugation and sonication steps in DCM to remove excess dichlorotriazinyl derivatives. This was followed by stirred-cell dialysis to remove inorganic base and any leftover unbound derivatives in the presence of acetone (3 cycle runs), acetone−water (50%, 3 cycle runs), and water (14 cycle runs). In method 2, since compound **4** is hydrophilic in nature, the solvent-exchange procedure in method 1 was not necessary, and the grafting reaction was carried out in a 70% water−acetone system. Compound **4** (5 mmol) in acetone (20 mL) was added to a stirred suspension containing CNCs in Milli-Q water (0.5 g, 1 wt %). Then, NaOH (10 mL, 0.2 N) was added to the mixture dropwise over 30 min and left to react under continuous stirring at room temperature for 24 h. A similar cleanup procedure as method 1 above was utilized for **DTAPEG**-modified CNCs.

**Fluorescein Labeling of Nanocellulose by an Azide−Alkyne Click Reaction.** See Scheme 1c. An aqueous suspension of BMCC (10 mL 0.3 wt %) was solvent-exchanged by successive centrifugation (10 000*g*, 5 °C, 5 min) and resuspension in acetone and then dry DCM, with sonication (10 min, 5 °C) in between each solvent-exchange step to prevent BMCC aggregation. $K_2CO_3$ was added (15 mg, 0.11 mmol) to a stirred suspension containing BMCC (30 mg, 0.3 wt %) in dry DCM (10 mL). After 20 min, compound **2** (30 mg, 0.15 mmol) in dry DCM (2 mL) was added and left to stir at room temperature for 24 h. Modified BMCC was then subjected to 3 successive centrifugation and sonication steps in DCM to remove excess **DTP** derivatives. This was followed by stirred-cell dialysis to remove inorganic base and any leftover unbound derivatives in the presence of acetone (3 cycle runs), acetone−water (50%, 3 cycle runs), and water (14 cycle runs). The modified BMCC was then used in the azide−alkyne click reaction as follows. A solution containing 5-FAM-azide (2 mg, 4.36 $\mu$mol) in ethanol (1 mL) was added to a stirred suspension containing **DTP**-modified BMCC (6 mg) in Milli-Q $H_2O$ (2 mL), followed by the addition of a solution containing $CuSO_4{\cdot}5H_2O$ (0.2 mg) and ascorbic acid (0.6 mg) in Milli-Q $H_2O$ (100 $\mu$L). The reaction mixture was stirred overnight in the dark at room temperature. The fluorescently labeled BMCC was cleaned-up with Milli-Q water through stirred-cell dialysis until the effluent gave a UV absorbance value similar to that of water.

## RESULTS AND DISCUSSION

**Triazine-Coordinated Chemical Grafting onto Nanocellulose.** Cyanuric chloride was utilized as a linker to tune the interfacial properties of nanocellulose in a modular fashion. In the synthetic approach, one of the three chlorine atoms of cyanuric chloride was substituted with octadecylamine (**DTC18**, **1**), propargylamine (**DTP**, **2**), benzylamine (**DTB**, **3**), or poly(ethylene glycol) monoallyl ether (**DTAPEG**, **4**), to yield four distinct triazinyl derivatives (Scheme 1a) with different physicochemical characteristics. After thorough characterization of the derivatives (NMR and MS spectra presented in Figures S1−S4), the triazine chemistry on cellulose was first demonstrated by grafting **DTC18** onto filter paper. This one-step reaction proceeded rapidly at room temperature and allowed us to tune the hydrophilicity of the cellulose surface (Figure 1). Under the reaction conditions selected for the triazine substitution, the filter paper presented water contact angles of


DOI: 10.1021/acs.chemmater.8b00511
*Chem. Mater.* 2018, 30, 2424−2435

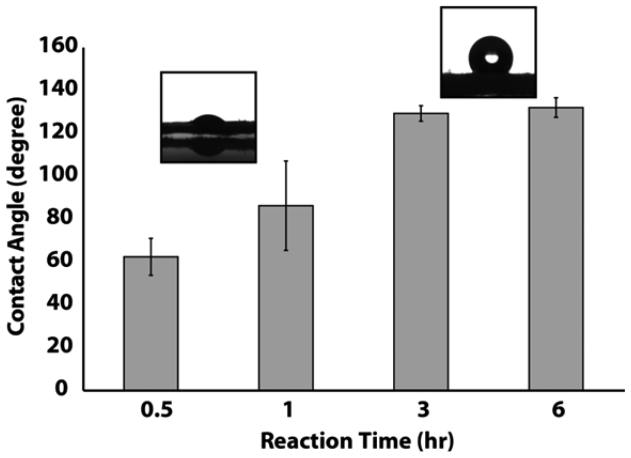


**Figure 1.** Tunable hydrophobization of filter paper through the controlled grafting of **DTC18** derivatives. Insets show the sessile water droplet contact angle measured on the filter paper after treatment. Error bars represent the standard deviation, $n = 3$.

~125° after 3 h. The contact angle did not increase even after doubling the reaction time, which points to a saturation of the cellulose surface with **DTC18**. Furthermore, it was observed that the water droplets remained intact on the surface of the modified paper even after prolonged incubation, indicating that the surface functionalization turned the filter paper into an effective water barrier. However, plasma oxidation of the modified cellulose surface returned the filter paper to a hydrophilic state, allowing full penetration of the water droplet into the filter lumen. These results show that the triazine chemistry can be used to tune the interfacial properties of cellulosic materials, where a **DTC18**-based modification can be used to define hydrophilic/hydrophobic areas, with application in the fabrication of channels for paper-based microanalytical devices.

Having demonstrated the triazine-mediated grafting for macroscopic cellulosic materials, we focused our attention on the surface modification of CNCs. The chemical modification of CNCs with nonpolar moieties presents a challenge, due to the charge imparted by the sulfate half-ester groups introduced during the production of CNCs via sulfuric acid hydrolysis.[9,28] Therefore, for the successful grafting of **DTC18**, **DTP**, and **DTB** onto CNCs, an initial solvent exchange was performed from an aqueous suspension to dichloromethane (DCM). This enabled the chemical modification of CNCs without aggregation using nonpolar triazinyl derivatives **1**, **2**, and **3** at ambient temperature in the presence of solid potassium carbonate as a hydrochloric acid scavenger (Scheme 1b). Conversely, the chemical grafting of **4** (a polar triazinyl derivative) onto CNCs was carried out in a straightforward fashion in aqueous solutions, where sodium hydroxide was used as the base. The etherification of CNCs by the triazinyl derivatives involved the nucleophilic aromatic substitution of the chlorine atoms present in compounds **1**–**4** by the numerous surface hydroxyl groups along the crystalline cellulose backbone. It has been reported that the ether linkages are stable, as shown by the imaging of bacterial cellulose microfibrils and CNCs fluorescently labeled with DTAF (dichlorotriazinyl-aminofluorescein).[25,31−33] To ensure that no unbound triazinyl derivatives were nonspecifically adsorbed onto the CNCs after the modification reactions, they were subjected to a rigorous cleanup procedure involving several washing steps through centrifugation (to remove the bulk of the unreacted material and base), followed by several cycles of stirred-cell dialysis. This cleanup procedure has been previously shown as an effective way to obtain reproducible and predictable DTAF grafting results.[33]

FTIR spectroscopy was used to confirm the covalent grafting of the triazinyl derivatives onto CNCs. Figure 2 shows a

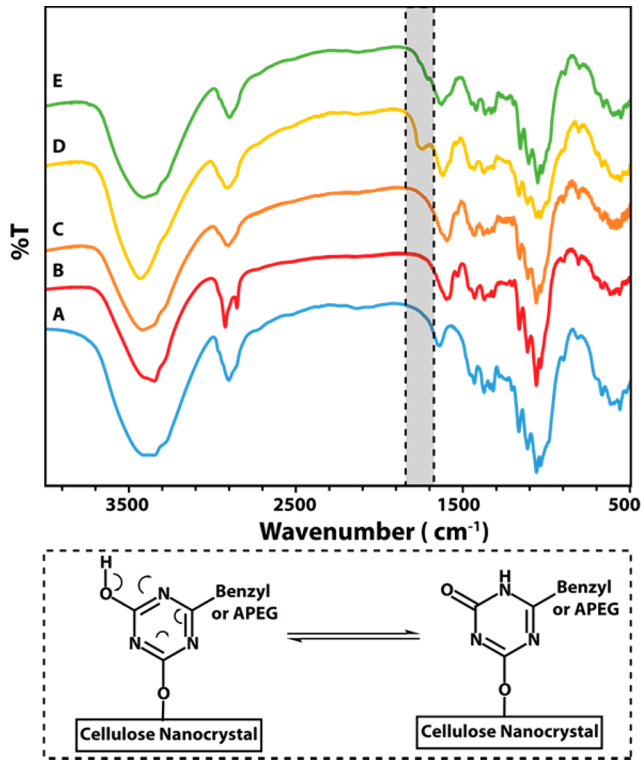


**Figure 2.** FTIR spectra of (A) unmodified CNC and (B–E) modified CNCs. The modified CNCs bear (B) **DTC18**, (C) **DTP**, (D) **DTB**, and (E) **DTAPEG** moieties. Inset shows the triazine ring tautomeric shift in **DTB**- and **DTAPEG**-modified CNCs.

comparison between the FTIR spectra of unmodified and chemically modified CNCs, demonstrating the successful grafting of C18, APEG, propargyl, and benzyl functionalities onto CNCs. The data show the appearance of distinct and unique absorption bands around 1630–1560 $cm^{-1}$ in each modified sample, which correspond to the C═N and C—N $sp^2$ vibrations present in the triazine rings chemically grafted onto CNCs. The modified CNCs also exhibit a narrower OH stretching band (3360 $cm^{-1}$) with broad shoulders (overlapping N—H, C≡C—H, and C═C—H stretching vibrations 3300–3010 $cm^{-1}$) due to the depletion of hydroxyl groups and the introduction of new chemical bonds at the cellulose surface. In addition, the appearance of characteristic aliphatic C—H stretching absorption bands (2960–2850 $cm^{-1}$) in modified CNCs (most prominent in C18) further confirms chemical grafting of the different triazinyl derivatives onto CNCs. It is also worth noting that a tautomeric shift within the triazine ring is observed in both benzyl-modified (prominent) and APEG-modified (minor) CNCs, which corresponds to the formation of amide bonds (1725 $cm^{-1}$, new C═ONH vibrations) with $\alpha,\beta$-unsaturation. This results from the substitution of the last chlorine atom (6-Cl) in the 4,6-dichlorotriazinyl derivatives by a hydroxyl group after initial chemical grafting onto the CNCs that, in turn, involves the shift of a proton from the introduced OH (enol form) to one of the adjacent nitrogen atoms. The outcome is a delocalization of the $\pi$-electrons within the triazine ring to


DOI: 10.1021/acs.chemmater.8b00511
Chem. Mater. 2018, 30, 2424–2435

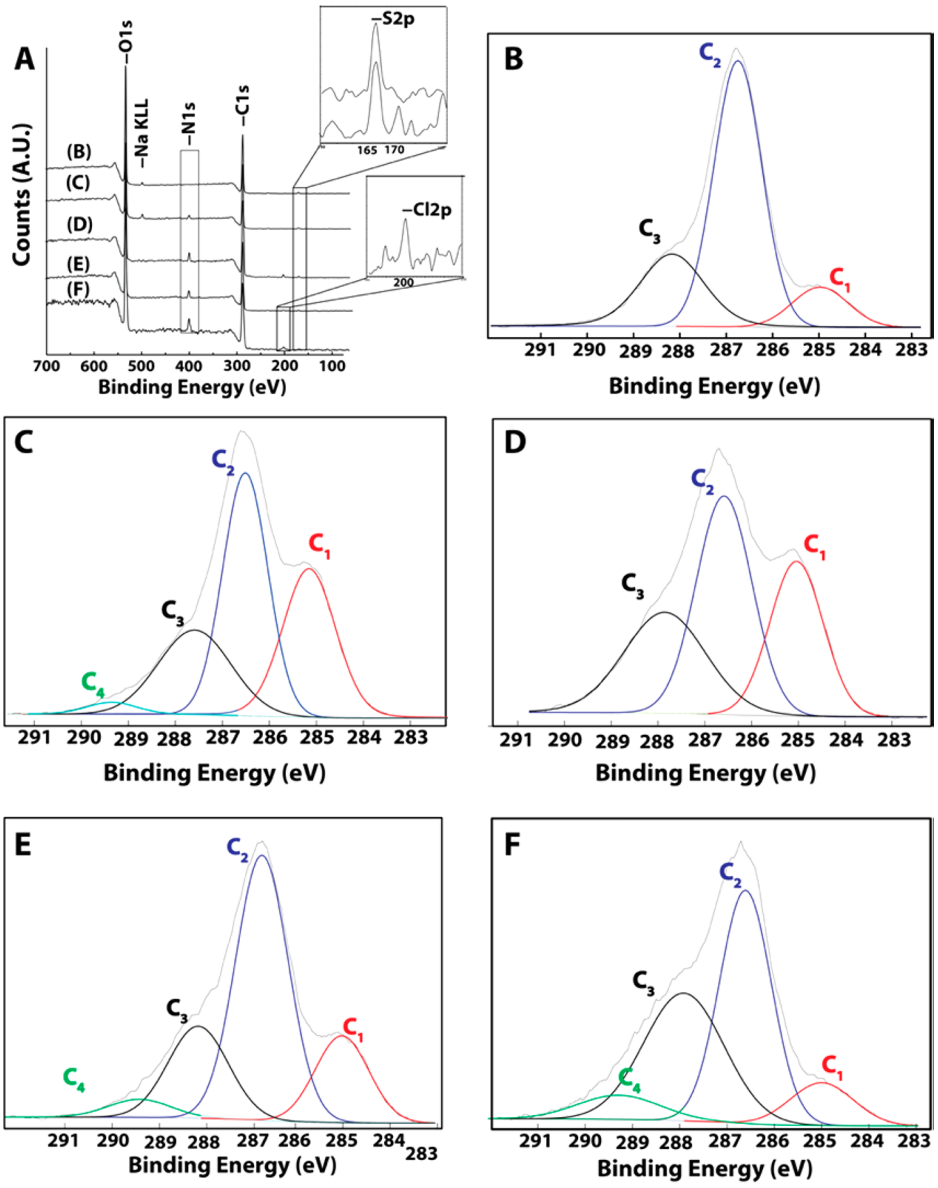


**Figure 3.** (A) Low-resolution XPS spectra, and high-resolution C 1s peak deconvolution of (B) unmodified CNC and CNCs modified with (C) **DTAPEG**, (D) **DTC18**, (E) **DTB**, and (F) **DTP**. Insets in panel a show the S 2p and Cl 2p signals, respectively, indicating the presence of sulfur and chlorine.

form amide bonds (keto form, Figure 2). This phenomenon was found to occur while drying the modified CNCs at elevated temperatures, as any bound water molecule can force the substitution of the third chlorine atom, hence the tautomeric shift into its most stable form.[34,35]

**Surface Grafting Efficiency of Triazinyl-Modified CNCs.** The surface modification efficiency of the triazine chemistry was established using X-ray photoelectron spectroscopy (XPS) and elemental analysis (EA), while X-ray diffraction (XRD) measurements were used to establish the retention of the crystallinity of unmodified and modified CNCs. Full scan low-resolution XPS spectra are shown in Figure 3a, highlighting the characteristic peaks observed around binding energies 287 and 534 eV, which correspond to carbon and oxygen atoms, respectively, as the main components in the anhydroglucose units of cellulose. The value of 0.80 oxygen-to-carbon (O/C) ratio (Table S1) for unmodified CNCs is close to those reported for pure cellulose.[36] As expected, the O/C ratios for all triazinyl-modified CNCs decreased in comparison to those for unmodified CNCs, a clear demonstration of the increase in carbon content as chemical modification was carried out. A small amount of sulfur was also detected at ~168 eV, which arose from sulfate half-ester groups grafted onto CNCs during production via sulfuric acid hydrolysis. In addition, modified CNCs exhibited distinct peaks at 400 and 200 eV, corresponding to nitrogen (N) and chlorine (Cl) atoms, respectively, that are non-native to cellulose. These new chemical signatures arise from the successful grafting of triazinyl derivatives and were consistently seen in all modified CNCs, with the exception of **DTAPEG**-CNCs where chlorine was not present in a detectable amount. This finding can be explained by the displacement of all chlorine atoms on the triazine ring when the grafting reaction was performed under basic conditions in an aqueous environment. Under these conditions, the last remaining chlorine atom could be displaced via hydrolysis after the initial **DTAPEG** grafting. The low-


DOI: 10.1021/acs.chemmater.8b00511
*Chem. Mater.* 2018, 30, 2424−2435

**Table 1. CNC Characterization**[a]

| sample | %C (corrected) | %H | %N | %S | DS | CI (%) | length (nm) | AHPR (nm) |
|---|---|---|---|---|---|---|---|---|
| CNCs | 41.28 (44.44) | 6.07 | 0.05 | 0.72 | | 95 ± 1 | 150 ± 40 | 90 ± 40 |
| **DTAPEG**-CNCs | 42.41 (45.67) | 6.37 | 1.88 | 0.65 | 0.06 ± 0.01 | 90 ± 4 | 150 ± 30 | 130 ± 40 |
| **DTB**-CNCs | 44.26 (47.67) | 5.95 | 2.50 | 0.70 | 0.16 ± 0.01 | 87 ± 1 | 140 ± 30 | 140 ± 50 |
| **DTP**-CNCs | 42.49 (45.76) | 5.81 | 3.70 | 0.73 | 0.18 ± 0.04 | 87 ± 3 | 170 ± 30 | 240 ± 120 |
| **DTC18**-CNCs | 46.13 (49.68) | 7.08 | 2.54 | 0.59 | 0.110 ± 0.003 | 78 ± 4 | 280 ± 80 | 300 ± 100 |

[a]The composition of all CNC materials was determined by elemental analysis (corrected values in parentheses). CNC crystallinity index (CI) was quantified by X-ray diffraction. CNC lengths were obtained from AFM images (histograms shown in Figure S5). The apparent hydrodynamic particle radius (AHPR) was obtained from DLS measurements (representative measurements shown in Figure S5). Values for all measurements are means of $n > 3$ replicate samples, except for AFM, where $n > 50$ particles were measured. Errors represent standard deviations.

resolution XPS results thus confirmed the surface grafting of triazinyl derivatives onto CNCs.

An additional advantage of XPS analysis is that detailed information about the surface chemistry of modified CNC can be retrieved from the deconvolution of high-resolution (surface) C 1s signals. The high-resolution C 1s spectra from unmodified and modified CNCs were deconvolved into the various carbon peaks, which reflect their local environments. The C1, C2, C3, and C4 peaks, with corresponding bond energies of 285.0, 286.3, 287.7, and 288.9 eV, were assigned to C—C/C—H aliphatic linkages, C—O linkages in alcohols and ethers, O—C—O/C═O linkages in acetals, and O—C═O linkages in esters, respectively.[28,36] Changes in the intensities of the C 1s signals (Figure 3) reflect changes in the relative proportions of the (surface) chemical bonds involving carbon atoms (including new types of bonds) associated with the grafted triazinyl derivative. A marked increase in C1 intensity was observed for **DTC18**-CNCs and **DTAPEG**-CNCs, confirming the successful grafting of aliphatic/ethylene chains onto CNCs through the triazine chemistry. On the other hand, only a small increase was recorded for benzyl- and propargyl-grafted CNCs, since their aliphatic/C—C bond contribution is minimal. All modified CNCs showed an expected increase in C3 peak intensity, which results from the new O—C═N or N—C═N bonds introduced by the covalent linkage between the triazinyl derivatives and the CNC surface.

While the low-resolution XPS results corroborate the presence of nitrogen and chlorine on modified CNCs, it was impossible to reliably determine the degree of surface substitution from the high-resolution data since the binding energies of the newly introduced O—C═O and N—C═N bonds overlap with those of acetal groups present in unmodified CNCs. Thus, elemental analysis was carried out to determine the degree of substitution (DS) in modified CNCs. DS values were calculated for modified CNCs from their relative atomic compositions (C, H, N, and S presented in Table 1) according to eq 1. A corrected carbon content was used in the calculation to account for the difference between the theoretical value (44.44%) and the experimentally obtained value (41.28%) for unmodified CNCs, which is in line with reported values.[28,29] The difference between theoretical and experimental values is ascribed to organic impurities adsorbed onto the surface of CNCs during storage or processing. A significant increase in nitrogen content over the baseline of unmodified CNCs was observed in all modified materials, as expected from the introduction of the triazinyl moiety. In addition, small amounts of sulfur from sulfate half-ester groups were observed in all samples, indicating that no significant desulfation occurred during the grafting procedure. The relative decrease in %S for modified CNCs, most noticeable in those bearing the bulkier **DTC18** and **DTAPEG** derivatives, was expected as a result of the proportional increase in C, H, and N content from the grafted triazinyl derivatives. The numbers of triazinyl derivatives grafted per 100 anhydroglucose units, as calculated from the carbon elemental analysis data, were 11, 18, 16, and 6 for **DTC18**-, **DTP**-, **DTB**-, and **DTAPEG**-grafted CNCs, respectively. These numbers correspond to 4−6% of the hydroxyl groups bearing triazine ether linkages in **DTC18**-, **DTP**-, and **DTB**-modified CNCs, and 2% in the case of **DTAPEG** grafting. The DS values reported here correspond to a high grafting efficiency, and are comparable to values reported for other chemistries used in the surface modification of CNCs.[37,38] Furthermore, the DS could be tuned by modifying the grafting conditions to tune the surface energy of CNCs, since only a small number of grafted molecules are needed to modify the interfacial properties of CNCs.[39]

**Structural Characterization of Modified Cellulose Nanocrystals.** X-ray diffraction (XRD) measurements were performed to assess the crystallinity of native and modified CNCs. The crystallinity index (CI) was determined using 2-dimensional diffraction intensity patterns (Figure S6). Integration along the relative angle $\chi$ for every $2\theta$ value was performed to obtain one-dimensional plots of intensity versus $2\theta$. Background corrected intensity versus $2\theta$ plots for native CNCs were then fitted to five symmetric Lorentzian peaks, four peaks corresponding to the (100), (010), (002), and (040) crystalline planes,[30] and one broad amorphous peak fixed at 24.1°. The four crystalline peaks were used to create a base crystalline cellulose scattering function, and the CI was calculated as the ratio of the area of this scattering function to the total area under the curve. This methodology has been previously validated against CNC−polymer mixtures with well-defined compositions.[40] This method yielded a CI value of 95% for unmodified CNCs (Table 1), which is in agreement with previous measurements.[40,41]

The scattering plots for CNCs modified with triazinyl derivatives (Figure S6) were then fitted to the base crystalline scattering function, where only the overall amplitude of the function was allowed to vary. This allowed the crystalline signal to be fitted keeping the relative proportion of each of the four crystalline peaks found in native CNCs constant. This practice was important because the triazinyl modifications could introduce signals that overlapped with the crystalline peaks and could bias the calculated crystallinity if each one of the crystalline peaks was fitted independently. The CI for the modified materials was then calculated as the ratio of the area under the crystalline scattering function over the total area under the curve. In all cases, it was observed that the introduced triazinyl modification moderately lowered the CI value (Table 1), since the grafted materials contributed to the signal considered amorphous. The changes in crystallinity were dependent not only on the degree of substitution, but also on the size of the



DOI: 10.1021/acs.chemmater.8b00511
Chem. Mater. 2018, 30, 2424−2435

grafted molecule, as made evident by the largest decrease for **DTC18**-grafted CNCs. A quick calculation using published values for CNC length and width (130 and 8 nm, respectively),[41] and crystalline cellulose density (1.5 g $cm^{-3}$),[42] and using the degree of substitution obtained from elemental analysis (Table 1), indicated that the mass of the crystalline cellulose core would represent ~79% of the total mass of the **DTC18**-modified nanoparticles. This is in good agreement with the CI values obtained from XRD, suggesting the crystallinity of the core CNCs was not affected by the modification, and that the changes in the scattering intensity arise solely from the surface grafting of the triazinyl derivatives.

AFM imaging was performed on dilute spin coated samples of the unmodified and modified CNCs to confirm the individual nature of the nanoparticles. Figure 4 shows that the native CNCs,

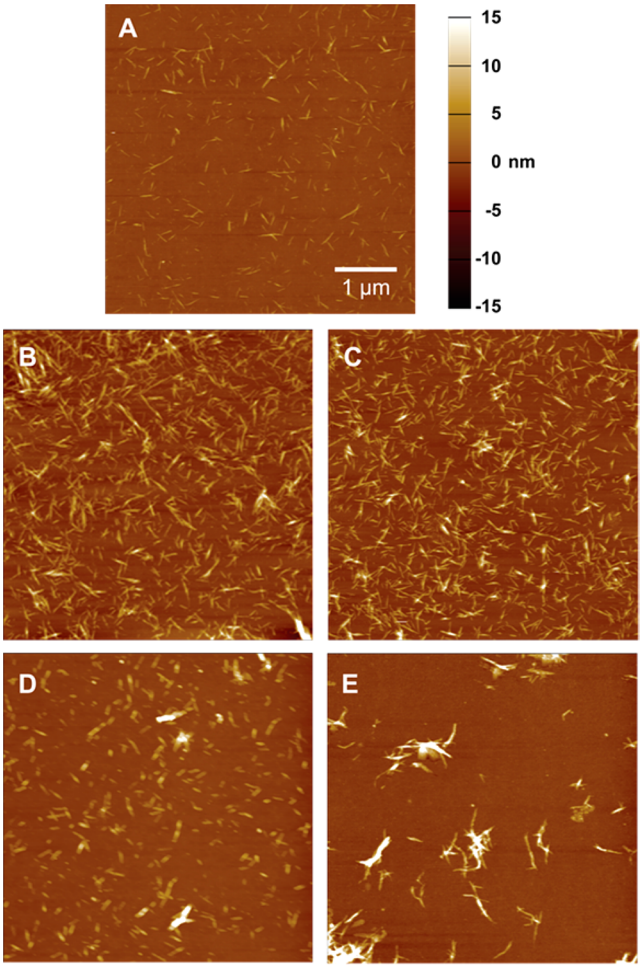


**Figure 4.** AFM height images of (A) unmodified CNC and CNCs modified with (B) **DTAPEG**, (C) **DTB**, (D) **DTP**, and (E) **DTC18**. All images acquired at the same magnification.

as well as those modified with **DTAPEG**, **DTB**, and **DTP**, appear well-dispersed and can be identified as individual particles, with only a few aggregates appearing in the modified materials, and being more predominant in the **DTP** sample. On the other hand, CNCs modified with **DTC18** showed a proportion of the sample in the form of submicron aggregates, where multiple individual particles could be visualized. Quantification of the length of the particles in the AFM images confirmed the visual observations, and yielded histograms with narrow dispersions for CNCs bearing **DTAPEG**, **DTB**, and **DTP**, and a wider distribution of sizes for those modified with **DTC18** (Figure S5). The averages and standard deviations for samples measuring $n > 50$ particles are presented in Table 1.

**Thermal Stability of Triazinyl-Modified CNCs.** The thermal degradation of CNCs during nanocomposite processing can severely limit their applicability. Thus, maintaining thermal stability after surface modification is a key requirement for the use of modified CNCs. Thermogravimetric analysis (TGA) was performed on unmodified and modified CNCs to study the effect that the chemically grafted triazinyl derivatives have on stability. The unmodified CNCs showed a thermal degradation profile characteristic to commercial CNCs[41] (sodium salt form) with the onset of degradation occurring at ~300 °C and the fastest degradation at ~330 °C (Figure 5). We observed that all

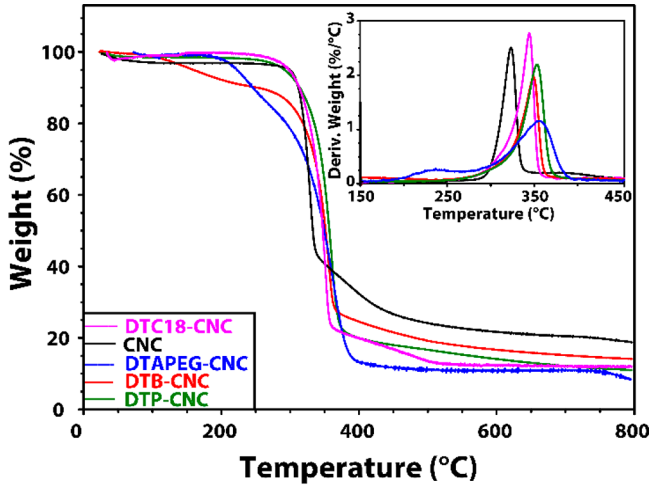


**Figure 5.** TGA thermograms and derivative curves (inset) of unmodified and modified CNCs.

modified materials had a similar onset, but showed a slight enhancement in thermal stability, as made evident by the fastest degradation of the cellulose core observed at ~350, 355, 360, and 365 °C for **DTC18**-, **DTB**-, **DTP**-, and **DTAPEG**-grafted CNCs, respectively (Figure 5, inset). This indicates that the sulfate half-ester groups on the backbone of the crystalline cellulose are further protected by the surface modification with the triazinyl derivatives. Nevertheless, the **DTAPEG**-modified particles showed partial degradation at lower temperatures, which is ascribed to the degradation of the grafted polymer chain, whose thermal stability is lower.

**Dispersion of Modified CNCs in Aqueous/Organic Media.** One of the goals of this work was to enhance the dispersion and stability of CNCs in a wide range of solvents through their modification with triazinyl derivatives. The blending of CNCs into materials for the formation of nanocomposites benefits from the compatibilization of the CNC surface chemistry with the receiving matrix, which ensures reduced aggregation, more uniform dispersion, and better transfer of the intrinsic CNC properties to the composite. To demonstrate this, the modified CNCs were dispersed in aqueous and organic media, and the suspensions were followed over time to investigate the impact of the introduced surface functionalities on the stability of the suspensions. Unmodified and modified CNCs were dispersed in solvents at a concentration of 0.5 wt % through 15 min point probe sonication in an ice bath. Figure 6


DOI: 10.1021/acs.chemmater.8b00511
Chem. Mater. 2018, 30, 2424−2435

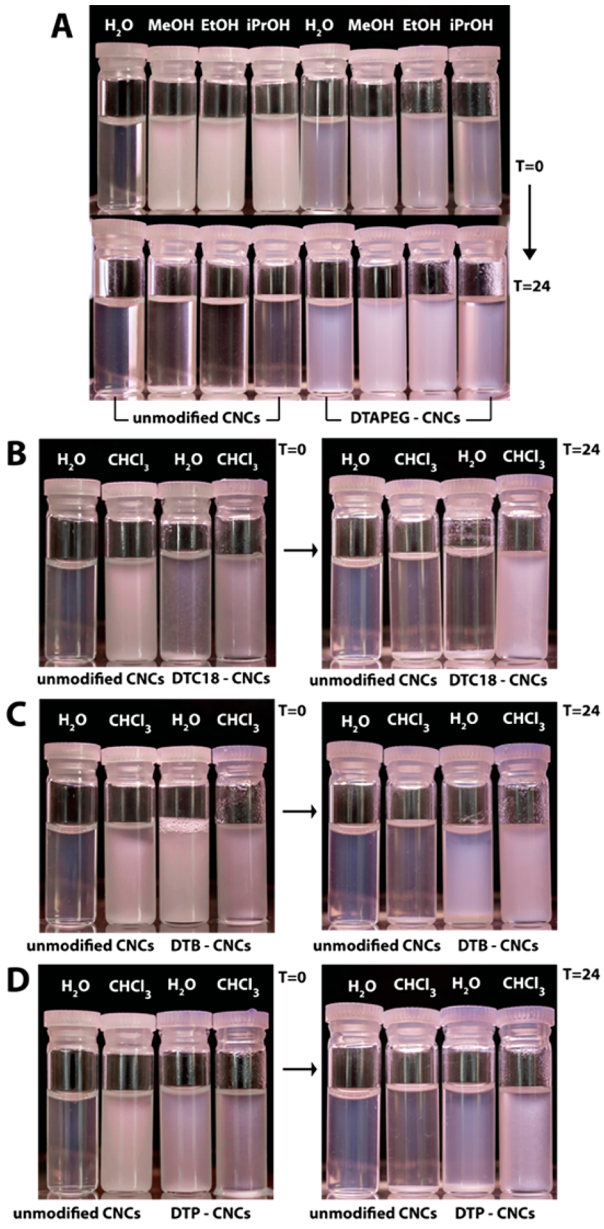


**Figure 6.** Photographs of unmodified and modified CNCs suspensions (0.5 wt %) in aqueous and organic media at $T$ = 0 h and $T$ = 24 h after sonication. (A) **DTAPEG**-CNCs, (B) **DTC18**-CNCs, (C) **DTB**-CNCs, and (D) **DTP**-CNCs.

shows pictures of the suspensions obtained immediately after sonication ($T$ = 0 h) and after being left undisturbed on the benchtop for 24 h. It was observed that **DTAPEG**-CNCs were dispersible in aqueous and polar organic solvents (methanol, ethanol, and isopropyl alcohol), and yielded homogeneous suspensions that remained stable over time through electrostatic and steric interactions. In contrast, unmodified CNCs almost immediately aggregated and crashed out of all polar solvents, with the exception of water. Further characterization through DLS (Table 1 and Figure S5) showed that unmodified CNCs and APEG-modified CNCs remained suspended as individual particles, with average hydrodynamic radii of 90 and 140 nm, respectively. The lack of noticeable aggregation, from DLS and AFM measurements, supports the notion of colloidal stabilization through steric and electrostatic repulsion. Thus, the introduction of polar polyether chains in the **DTAPEG** derivative made the CNCs stable and compatible with water and polar organic solvents.

Similarly, the grafting of **DTC18**, **DTB**, and **DTP** introduced alkyl, benzyl, and propargyl moieties, respectively, that rendered the CNCs hydrophobic. Consequently, CNCs modified with such triazinyl derivatives were dispersible and remained stable in chloroform, while unmodified CNCs immediately aggregated and crashed out of this solvent. On the other hand, when suspended in water, **DTC18**-CNCs rapidly crashed out of solution, while **DTB**-CNCs and **DTP**-CNCs showed moderate stability and slow sedimentation. Further characterization through DLS showed that **DTB** showed similar characteristics to unmodified CNCs and **DTAPEG**-modified CNCs. On the other hand, the average apparent hydrodynamic radii of **DTP** and **DTC18** were 2−3-fold larger than those of unmodified CNCs, which suggests short-range clustering of the modified CNCs over time. This confirmed the observations from AFM images of **DTC18**-CNCs (Figure 4E), where small clusters were easily discernible. Despite the short-range clustering observed, the introduction of **DTB**, **DTP**, and **DTC18** modifications made the CNCs compatible with nonpolar organic solvents. It must be highlighted that those suspensions, exhibiting stability after 24 h, were found to remain stable even after months of storage in appropriately sealed containers. The compatibilization of modified CNCs with a range of organic solvents could open the door for their use as fillers and reinforcing agents in a range of polymeric and nonpolymeric matrices.

**Fluorescent Labeling of DTP-Modified Cellulose Fibers through "Click" Reactions.** Finally, as proof-of-concept, we aimed to demonstrate the versatility of the triazine chemistry by using it as a modular platform for the secondary modification of crystalline cellulose through "click" chemistry. To this end, we first grafted **DTP** onto bacterial microcrystalline cellulose (BMCC) fibrils to introduce alkyne functionalities and carried out a secondary azide−alkyne cycloaddition reaction with azido-fluorescein (Scheme 1c). This yielded uniformly and brightly labeled BMCC fibrils that could be readily imaged through fluorescence microscopy (Figure 7). This procedure not only demonstrates the ability to use the triazinyl chemistry as a building block for secondary modifications, but also opens the

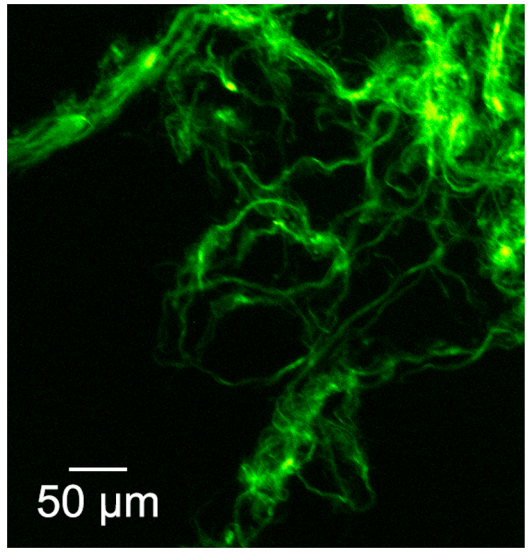


**Figure 7. DTP**-grafted BMCC fibrils labeled through a secondary azide−alkyne cycloaddition reaction with fluorescein derivatives.


DOI: 10.1021/acs.chemmater.8b00511
Chem. Mater. 2018, 30, 2424−2435

**Table 2. Comparison of Different Chemistries Used in the Modification of Nanocellulose Surfaces**

| strategy | process considerations | reaction conditions | refs |
|---|---|---|---|
| acetylation | Reaction involves low-cost reagents, and products are stable. However, reaction conditions are highly susceptible to "peeling effect" of CNCs, where the CNS crystalline structure/morphology is adversely affected. Reaction/degree of substitution are difficult to control. Only acetylated CNCs are produced, no route for selective postmodification. | 94 °C, inert atmosphere, DMF, $K_2CO_3$, 1−24 h | 43 |
| esterification (ring-opening and ATRP polymerization) | Reaction involves high-cost reagents (alkenyl succinic anhydrides) and involves a freezing drying step before modification. Approach available for the modification of CNCs with alkenyl succinic anhydrides. | 105 °C for 2 min | 44 |
| | Reaction involves high-cost reagents (lactide, tin catalyst), and requires solvent exchange and distillation. The reaction allows grafting of polymer chains through ROP from CNCs. | 80 °C, inert atmosphere, dry toluene, 24 h | 45 |
| | Reaction involves a laborious two-step process that uses high-cost reagents (2-bromoisobutyryl bromide, Cu(I)Br, styrene, MMAZO, etc.) and involves freeze−thaw cycles before modification. The resulting materials can be used to graft polymer chains from the CNC surface through ATRP. | room temperature (RT), DMAP, TEA, dry THF, 24 h; 110 °C, HMTETA, neat, 12 h; 90 °C, chlorobenzene, HMTETA, 24 h | 18, 19 |
| silylation | Simple and versatile procedure, with many potential functionalities through commercially available silanes. Reaction involves very costly reagents (chloro/alkoxysilanes) that could make it prohibitive for large-scale applications. Solvent exchange is required when using chlorosilanes and a freeze-drying step in addition to an annealing process is necessary when using alkoxysilanes. Cellulose crystallinity could be modified during the silylation process. | RT, dry toluene, imidazole, 16 h; RT, $H_2O$, 2−4 h, 110 °C, 8 h | 46, 47; 48, 49 |
| amidation/carbamination | Reaction involves a laborious two-step process, where the CNC is first oxidized, and then EDC coupling is performed. The process involves high-cost reagents (TEMPO, NaClO, EDC, NHS, etc.), and the degree of oxidation must be carefully controlled. Depending on the functionality introduced, the CNC may require solvent exchange before modification. | RT, $H_2O$, DMF, pH = 7.5−8; 2−4 h | 16, 17 |
| | Reaction involves a laborious one-/three-step process. The process involves costly reagents (isocyanates-phNCO, diisocyanates-2,4-TDI). The procedure requires solvent exchange before CNC modification. Allows grafting well-defined, amine-terminated polymers onto CNCs without modification of the CNC crystallinity. | 80−110 °C, inert atmosphere, TEA, from 30 min to 7 days | 12−14 |
| etherification | The reaction is simple to implement, but the cost depends on the epoxide used for modification. Complete activation of surface hydroxyl groups with basic solutions required for efficient functionalization. Base content used needs to be carefully controlled to avoid loss of crystallinity. May require a desulfation step before modification reaction. | 65 °C, $H_2O$, NaOH, 5−6.5 h | 11, 20 |
| triazinyl | The reaction is simple, is performed under mild conditions, and involves low-cost reagents (cyanuric chloride < $10/kg), and the resulting products are stable. The process is highly tunable, and the resulting modified cellulose/CNCs can be either polar or nonpolar and amenable to postfunctionalization. Depending on the functionality introduced, the CNC may require solvent exchange before modification. | RT, $H_2O$/acetone, NaOH, 24 h; RT, DCM, $K_2CO_3$, 24 h | this work |



DOI: 10.1021/acs.chemmater.8b00511
Chem. Mater. 2018, 30, 2424−2435

possibility of designing heterobifunctional triazinyl derivatives where one functionality can be used for solvent compatibilization and the second for targeted reactions. Our group is currently pursuing a number of cellulose modification routes along this direction.

**Triazinyl Chemistry Cellulose Modification in Context.** The discussion so far has focused on the effectiveness of the triazinyl chemistry approach to modify the interfacial properties of cellulose with a range of functional moieties. However, to place this chemistry into proper context, one must compare it with other available surface modification approaches. Table 2 compares some of the cellulose modification strategies reported to date, detailing process considerations and reaction conditions obtained from the cited references. While this comparison does not aim to be exhaustive, it provides representative examples, and highlights some of the advantages of the triazinyl chemistry. In particular, the surface modification of cellulose through the triazinyl chemistry is carried out under mild conditions that do not negatively impact the native structure of cellulose, is versatile in the types of functional groups that can be grafted onto the surface—ranging from polar to nonpolar and from small molecules to polymers, and can be carried out with inexpensive reagents. These considerations render the triazinyl chemistry a simple, versatile, and low-cost approach to carry out surface modification of nanocellulose with potential for large-scale implementation.

## CONCLUSIONS

In this work, we have introduced triazinyl chemistry as a versatile modular approach for tuning the interfacial properties of cellulosic materials using both "grafting to" and "grafting from" reactions. Cyanuric chloride, a relatively inexpensive chemical, was deployed as a linker molecule for the grafting of aliphatic (octadecylamine), polymeric (monoallyl PEG), aromatic (benzylamine), and alkyne (proparygyl) functionalities onto CNCs, forming stable cellulose ether derivatives. Depending on the functionality introduced, the triazine grafting technique was conducted in either aqueous or organic media. Colloidal suspensions of modified CNCs were easily generated and sterically stabilized in polar or nonpolar organic solvents. The ability to tune the polarity of the CNC surface is promising for their dispersion into hydrophilic and hydrophobic polymer matrices, and for their use as fillers and reinforcing agents for the generation of nanocomposites with unique mechanical, optical, and electrical properties. Finally, the postmodification of alkynyl-grafted CNCs was demonstrated through an azide−alkyne cycloaddition reaction, which was used to fluorescently label the modified cellulose nanofibers. This showcases the ability to use the triazinyl group as a modular building block for such bio-orthogonal reactions, and opens the way for the future development of heterobifunctional molecules for the incorporation of nanocellulose into a wide range of materials.

## ASSOCIATED CONTENT

### Supporting Information

The Supporting Information is available free of charge on the ACS Publications website at DOI: 10.1021/acs.chemmater.8b00511.

$^{1}$H and $^{13}$C NMR spectroscopy and mass spectrometry of 4,6-dichlorotriazinyl derivatives, XRD spectra obtained from unmodified and modified CNC materials, Elemental percentages present obtained from low-resolution XPS survey scan surface, functional group composition obtained from the deconvolution of the peak C 1s for unmodified and modified CNCs, and calculation and conversion of the degree of substitution (DS) to surface degree of substitution (DSS) (PDF)

## AUTHOR INFORMATION


### Corresponding Author

*E-mail: mirabj@mcmaster.ca.

### ORCID

Michael A. Brook: 0000-0003-0705-9657

Jose M. Moran-Mirabal: 0000-0002-4811-3085


### Notes

The authors declare no competing financial interest.

## ACKNOWLEDGMENTS

We thank Prof. E. Cranston and Prof. Alex Adronov for access to equipment and useful discussions, and V. Jarvis (McMaster Analytical X-ray Diffraction Facility) and D. Covelli (Biointerfaces Institute) for assistance with sample analysis. This research was supported through the Natural Sciences and Engineering Research Council and a Canada Foundation for Innovation Leaders Opportunity Fund. A.F. was partially supported by the BioInterfaces CREATE grant. J.M.M.-M. is the recipient of an Early Researcher Award from the Ontario Ministry for Research and Innovation, and the Canada Research Chair on Micro and Nanostructured Materials. We thank EnRoute Interfaces Inc. for providing poly(ethylene glycol) monoallyl ether.

## REFERENCES


(1) Peponi, L.; Puglia, D.; Torre, L.; Valentini, L.; Kenny, J. M. Processing of nanostructured polymers and advanced polymeric based nanocomposites. *Mater. Sci. Eng., R* **2014**, *85*, 1−46.

(2) Miao, C.; Hamad, W. Y. Cellulose reinforced polymer composites and nanocomposites: a critical review. *Cellulose* **2013**, *20*, 2221−2262.

(3) Moon, R. J.; Martini, A.; Nairn, J.; Simonsen, J.; Youngblood, J. Cellulose nanomaterials review: structure, properties and nanocomposites. *Chem. Soc. Rev.* **2011**, *40*, 3941−3994.

(4) Roman, M. Toxicity of Cellulose Nanocrystals: A Review. *Ind. Biotechnol.* **2015**, *11*, 25−33.

(5) Azzam, F.; Heux, L.; Putaux, J.-L.; Jean, B. Preparation By Grafting Onto, Characterization, and Properties of Thermally Responsive Polymer-Decorated Cellulose Nanocrystals. *Biomacromolecules* **2010**, *11*, 3652−3659.

(6) Dufresne, A. Processing of Polymer Nanocomposites Reinforced with Polysaccharide Nanocrystals. *Molecules* **2010**, *15*, 4111−4128.

(7) Yang, J.; Han, C.-R.; Duan, J.-F.; Ma, M.-G.; Zhang, X.-M.; Xu, F.; Sun, R.-C. Synthesis and characterization of mechanically flexible and tough cellulose nanocrystals-polyacrylamide nanocomposite hydrogels. *Cellulose* **2013**, *20*, 227−237.

(8) Azizi Samir, M. A. S.; Alloin, F.; Dufresne, A. Review of Recent Research into Cellulosic Whiskers, Their Properties and Their Application in Nanocomposite Field. *Biomacromolecules* **2005**, *6*, 612−626.

(9) Kan, K. H. M.; Li, J.; Wijesekera, K.; Cranston, E. D. Polymer-Grafted Cellulose Nanocrystals as pH-Responsive Reversible Flocculants. *Biomacromolecules* **2013**, *14*, 3130−3139.

(10) Ljungberg, N.; Bonini, C.; Bortolussi, F.; Boisson, C.; Heux, L.; Cavaillé. New Nanocomposite Materials Reinforced with Cellulose Whiskers in Atactic Polypropylene: Effect of Surface and Dispersion Characteristics. *Biomacromolecules* **2005**, *6*, 2732−2739.

(11) Hasani, M.; Cranston, E. D.; Westman, G.; Gray, D. G. Cationic surface functionalization of cellulose nanocrystals. *Soft Matter* **2008**, *4*, 2238−2244.




DOI: 10.1021/acs.chemmater.8b00511
*Chem. Mater.* 2018, 30, 2424−2435

(12) Habibi, Y.; Dufresne, A. Highly Filled Bionanocomposites from Functionalized Polysaccharide Nanocrystals. *Biomacromolecules* **2008**, *9*, 1974−1980.
(13) Siqueira, G.; Bras, J.; Dufresne, A. Cellulose Whiskers versus Microfibrils: Influence of the Nature of the Nanoparticle and its Surface Functionalization on the Thermal and Mechanical Properties of Nanocomposites. *Biomacromolecules* **2009**, *10*, 425−432.
(14) Shang, W.; Huang, J.; Luo, H.; Chang, P. R.; Feng, J.; Xie, G. Hydrophobic modification of cellulose nanocrystal via covalently grafting of castor oil. *Cellulose* **2013**, *20*, 179−190.
(15) Yu, H.-Y.; Chen, R.; Chen, G.-Y.; Liu, L.; Yang, X.-G.; Yao, J.-M. Silylation of cellulose nanocrystals and their reinforcement of commercial silicone rubber. *J. Nanopart. Res.* **2015**, *17*, 1−13.
(16) Mangalam, A. P.; Simonsen, J.; Benight, A. S. Cellulose/DNA Hybrid Nanomaterials. *Biomacromolecules* **2009**, *10*, 497−504.
(17) Harrisson, S.; Drisko, G. L.; Malmström, E.; Hult, A.; Wooley, K. L. Hybrid Rigid/Soft and Biologic/Synthetic Materials: Polymers Grafted onto Cellulose Microcrystals. *Biomacromolecules* **2011**, *12*, 1214−1223.
(18) Yi, J.; Xu, Q.; Zhang, X.; Zhang, H. Chiral-nematic self-ordering of rodlike cellulose nanocrystals grafted with poly(styrene) in both thermotropic and lyotropic states. *Polymer* **2008**, *49*, 4406−4412.
(19) Xu, Q.; Yi, J.; Zhang, X.; Zhang, H. A novel amphotropic polymer based on cellulose nanocrystals grafted with azo polymers. *Eur. Polym. J.* **2008**, *44*, 2830−2837.
(20) Kloser, E.; Gray, D. G. Surface Grafting of Cellulose Nanocrystals with Poly(ethylene oxide) in Aqueous Media. *Langmuir* **2010**, *26*, 13450−13456.
(21) Tappe, H.; Helmling, W.; Mischke, P.; Rebsamen, K.; Reiher, U.; Russ, W.; Schläfer, L.; Vermehren, P. Reactive Dyes. In *Ullmann's Encyclopedia of Industrial Chemistry*; Wiley-VCH Verlag GmbH & Co. KGaA, 2000.
(22) Müller, F.; Applebyki, A. P. Weed Control, 2. Individual Herbicides. In *Ullmann's Encyclopedia of Industrial Chemistry*; Wiley-VCH Verlag GmbH & Co. KGaA, 2000.
(23) Siegrist, A. E.; Eckhardt, C.; Kaschig, J.; Schmidt, E. Optical Brighteners. In *Ullmann's Encyclopedia of Industrial Chemistry*; Wiley-VCH Verlag GmbH & Co. KGaA, 2000.
(24) Chouai, A.; Simanek, E. E. Kilogram-Scale Synthesis of a Second-Generation Dendrimer Based on 1,3,5-Triazine Using Green and Industrially Compatible Methods with a Single Chromatographic Step. *J. Org. Chem.* **2008**, *73*, 2357−2366.
(25) Helbert, W.; Chanzy, H.; Husum, T. L.; Schülein, M.; Ernst, S. Fluorescent Cellulose Microfibrils As Substrate for the Detection of Cellulase Activity. *Biomacromolecules* **2003**, *4*, 481−487.
(26) Ringot, C.; Sol, V.; Barrière, M.; Saad, N.; Bressollier, P.; Granet, R.; Couleaud, P.; Frochot, C.; Krausz, P. Triazinyl Porphyrin-Based Photoactive Cotton Fabrics: Preparation, Characterization, and Antibacterial Activity. *Biomacromolecules* **2011**, *12*, 1716−1723.
(27) Walczak, M.; Frączyk, J.; Kamiński, Z. J.; Wietrzyk, J.; Filip-Psurska, B. Preliminary studies on application of library of artificial receptors for differentiation of metabolites in urine of healthy and cancer bearing mice. *Acta Polym. Pharm.* **2014**, *71*, 941−953.
(28) Siqueira, G.; Bras, J.; Dufresne, A. New Process of Chemical Grafting of Cellulose Nanoparticles with a Long Chain Isocyanate. *Langmuir* **2010**, *26*, 402−411.
(29) Ly, B.; Thielemans, W.; Dufresne, A.; Chaussy, D.; Belgacem, M. N. Surface functionalization of cellulose fibres and their incorporation in renewable polymeric matrices. *Compos. Sci. Technol.* **2008**, *68*, 3193−3201.
(30) Briois, B.; Saito, T.; Pétrier, C.; Putaux, J.-L.; Nishiyama, Y.; Heux, L.; Molina-Boisseau, S. I$\alpha \rightarrow$ I$\beta$ transition of cellulose under ultrasonic radiation. *Cellulose* **2013**, *20*, 597−603.
(31) Jasmani, L.; Eyley, S.; Wallbridge, R.; Thielemans, W. A facile one-pot route to cationic cellulose nanocrystals. *Nanoscale* **2013**, *5*, 10207−10211.
(32) Moran-Mirabal, J. M.; Santhanam, N.; Corgie, S. C.; Craighead, H. G.; Walker, L. P. Immobilization of cellulose fibrils on solid substrates for cellulase-binding studies through quantitative fluorescence microscopy. *Biotechnol. Bioeng.* **2008**, *101*, 1129−1141.
(33) Abitbol, T.; Palermo, A.; Moran-Mirabal, J. M.; Cranston, E. D. Fluorescent Labeling and Characterization of Cellulose Nanocrystals with Varying Charge Contents. *Biomacromolecules* **2013**, *14*, 3278−3284.
(34) Mur, V. I.; Levin, E. S.; Vinogradova, N. P. Synthesis and reactions of some substituted 1, 3, 5-triazines. *Chem. Heterocycl. Compd. (N. Y., NY, U. S.)* **1967**, *3*, 589−594.
(35) Bailey, J.; Kettle, L. J.; Cherryman, J. C.; Mitchell, J. B. O. Triazinone tautomers: solid phase energetics. *CrystEngComm* **2003**, *5*, 498−502.
(36) Zoppe, J. O.; Habibi, Y.; Rojas, O. J.; Venditti, R. A.; Johansson, L.-S.; Efimenko, K.; Österberg, M.; Laine, J. Poly(N-isopropylacrylamide) Brushes Grafted from Cellulose Nanocrystals via Surface-Initiated Single-Electron Transfer Living Radical Polymerization. *Biomacromolecules* **2010**, *11*, 2683−2691.
(37) de Mesquita, J. P.; Donnici, C. L.; Teixeira, I. F.; Pereira, F. V. Bio-based nanocomposites obtained through covalent linkage between chitosan and cellulose nanocrystals. *Carbohydr. Polym.* **2012**, *90*, 210−217.
(38) Lin, N.; Dufresne, A. Surface chemistry, morphological analysis and properties of cellulose nanocrystals with gradiented sulfation degrees. *Nanoscale* **2014**, *6*, 5384−5393.
(39) Peydecastaing, J.; Vaca-Garcia, C.; Borredon, E. Accurate determination of the degree of substitution of long chain cellulose esters. *Cellulose* **2009**, *16*, 289−297.
(40) Gill, U.; Sutherland, T.; Himbert, S.; Zhu, Y.; Rheinstadter, M. C.; Cranston, E. D.; Moran-Mirabal, J. M. Beyond buckling: humidity-independent measurement of the mechanical properties of green nanobiocomposite films. *Nanoscale* **2017**, *9*, 7781−7790.
(41) Reid, M. S.; Villalobos, M.; Cranston, E. D. Benchmarking Cellulose Nanocrystals: From the Laboratory to Industrial Production. *Langmuir* **2017**, *33*, 1583−1598.
(42) Dufresne, A. Nanocellulose: a new ageless bionanomaterial. *Mater. Today* **2013**, *16*, 220−227.
(43) Çetin, N. S.; Tingaut, P.; Özmen, N.; Henry, N.; Harper, D.; Dadmun, M.; Sèbe, G. Acetylation of Cellulose Nanowhiskers with Vinyl Acetate under Moderate Conditions. *Macromol. Biosci.* **2009**, *9*, 997−1003.
(44) Yuan, H.; Nishiyama, Y.; Wada, M.; Kuga, S. Surface Acylation of Cellulose Whiskers by Drying Aqueous Emulsion. *Biomacromolecules* **2006**, *7*, 696−700.
(45) Goffin, A.-L.; Raquez, J.-M.; Duquesne, E.; Siqueira, G.; Habibi, Y.; Dufresne, A.; Dubois, P. From Interfacial Ring-Opening Polymerization to Melt Processing of Cellulose Nanowhisker-Filled Polylactide-Based Nanocomposites. *Biomacromolecules* **2011**, *12*, 2456−2465.
(46) Pei, A.; Zhou, Q.; Berglund, L. A. Functionalized cellulose nanocrystals as biobased nucleation agents in poly(l-lactide) (PLLA) − Crystallization and mechanical property effects. *Compos. Sci. Technol.* **2010**, *70*, 815−821.
(47) Goussé, C.; Chanzy, H.; Excoffier, G.; Soubeyrand, L.; Fleury, E. Stable suspensions of partially silylated cellulose whiskers dispersed in organic solvents. *Polymer* **2002**, *43*, 2645−2651.
(48) Raquez, J. M.; Murena, Y.; Goffin, A. L.; Habibi, Y.; Ruelle, B.; DeBuyl, F.; Dubois, P. Surface-modification of cellulose nanowhiskers and their use as nanoreinforcers into polylactide: A sustainably-integrated approach. *Compos. Sci. Technol.* **2012**, *72*, 544−549.
(49) Huang, J.-L.; Li, C.-J.; Gray, D. G. Functionalization of cellulose nanocrystal films via "thiol-ene" click reaction. *RSC Adv.* **2014**, *4*, 6965−6969.


DOI: 10.1021/acs.chemmater.8b00511
*Chem. Mater.* 2018, 30, 2424−2435